



Atmospheric Iodine (^{127}I and ^{129}I) Record in Spruce Tree Rings in the Northeast Qinghai-Tibet Plateau

Zhao, Xue; Hou, Xiaolin; Zhou, Weijian

Published in:
Environmental Science and Technology

Link to article, DOI:
[10.1021/acs.est.9b01160](https://doi.org/10.1021/acs.est.9b01160)

Publication date:
2019

Document Version
Peer reviewed version

[Link back to DTU Orbit](#)

Citation (APA):
Zhao, X., Hou, X., & Zhou, W. (2019). Atmospheric Iodine (^{127}I and ^{129}I) Record in Spruce Tree Rings in the Northeast Qinghai-Tibet Plateau. *Environmental Science and Technology*, 53(15), 8706-8714.
<https://doi.org/10.1021/acs.est.9b01160>

General rights

Copyright and moral rights for the publications made accessible in the public portal are retained by the authors and/or other copyright owners and it is a condition of accessing publications that users recognise and abide by the legal requirements associated with these rights.

- Users may download and print one copy of any publication from the public portal for the purpose of private study or research.
- You may not further distribute the material or use it for any profit-making activity or commercial gain
- You may freely distribute the URL identifying the publication in the public portal

If you believe that this document breaches copyright please contact us providing details, and we will remove access to the work immediately and investigate your claim.

1 Atmospheric iodine (^{127}I and ^{129}I) record in spruce
2 tree rings in the northeast Qinghai-Tibet Plateau

3 *Xue Zhao*^{a,c,e}, *Xiaolin Hou*^{a,b,c,d*}, *Weijian Zhou*^{a,b,d}

4 a.State Key Laboratory of Loess and Quaternary Geology, Shaanxi Key Laboratory of
5 Accelerator Mass Spectrometry Technology and Application, Xi'an AMS Center, Institute
6 of Earth Environment, CAS, Xi'an 710061, China

7 b. CAS Center for Excellence in Quaternary Science and Global Change, Xi'an, 710061,
8 China

9 c. Technical University of Denmark, Center for Nuclear Technologies, Risø Campus,
10 Roskilde 4000, Denmark

11 d. Open Studio for Oceanic-Continental Climate and Environment Changes, Pilot National
12 Laboratory for Marine Science and Technology (Qingdao), Qingdao 266100, China

13 e. University of Chinese Academy of Sciences, Beijing 100049, China

* Corresponding author: Technical university of Denmark, Center for Nuclear Technologies, Frederiksborgvej 399, Roskilde 4000, Denmark. Tel.: +45-21325129; fax: +45-46775347; E-mail address: houxl@ieecas.cn (X. Hou).

14 **ABSTRACT:** Atmospheric iodine isotopes have significant impacts on climate change and
15 human health. However, the sources, transport pathway, and transfer process of atmospheric
16 iodine are still not well understood. Tree rings of spruce collected from the east edge of Qinghai-
17 Tibet Plateau were analyzed for iodine isotopes (^{127}I and ^{129}I). The results show that the levels
18 and temporal variation of atmospheric iodine were well recorded in the spruce tree rings, and
19 iodine concentrations in tree rings increased three times from 1960 to 2015, reflecting the
20 increased releases of iodine to the atmosphere in the past decades due to the human activities.
21 The anthropogenic ^{129}I in the tree rings presents the record of the human nuclear activities in the
22 past 55 years. The sources and the transport pathways of radioactive substances could be
23 extracted from the ^{129}I recorded in the tree rings in Qinghai-Tibet region. They are fallout of the
24 global nuclear weapons tests in 1961-1962, releases of the Chinese atmospheric nuclear weapons
25 tests in 1964-1980 transported through the tropospheric northwest wind, the releases of the
26 Chernobyl accident dispersed through Westerlies and the continuous air releases before 1997 and
27 the re-emission of marine discharges from the European nuclear fuel reprocessing plants
28 transported through Westerlies.

29 **Key words:** Atmospheric iodine, Iodine-129, source term, transport pathway, Spruce, Tree rings

30

31 **INTRODUCTION**

32 Iodine is an essential trace element of mammals. Iodine deficiency can result in irreversibly
33 neurological damage and developmental retardation in newborns. The major source of iodine in
34 terrestrial environment is from atmospheric deposition.¹ The atmospheric iodine has a significant
35 impact on climate through tropospheric ozone depletion and aerosol formation, and was

36 observed several times to be changed in recent decades.^{1,2,3} Although some investigations have
37 been carried out by measuring iodine in soil, sediment and ice cores,^{3,4} the sources, the transport
38 pathway and transfer process of atmospheric iodine in the ecosystem are still not well understood
39 due to its multi-sources and the difficulties on discrimination of the different sources.

40 ¹²⁹I, a long-lived radioisotope of iodine ($T_{1/2}=15.7$ Ma), has been released to the environment
41 by human nuclear activities, including nuclear fuel reprocessing plants (NFRPs), nuclear
42 weapons tests (NWTs) and nuclear accidents (NA). The anthropogenic ¹²⁹I (NFRPs: 7400 kg;
43 NWTs: 150 kg; NAs: 7.2 kg) has highly overwhelmed the natural inventory in surface
44 environment (250 kg, with a pre-nuclear ¹²⁹I/¹²⁷I atomic ratio of 1.5×10^{-12}).^{5,6} Due to unique
45 source of anthropogenic ¹²⁹I, volatile property and biophilic characteristics of iodine, the
46 anthropogenic ¹²⁹I has been widely applied as an environmental tracer for investigation of
47 regional radioactive sources and the related atmospheric transport pathways by determination of
48 ¹²⁹I preserved in time-serial samples (sediment, ice core and coral samples).⁶⁻¹² However, due to
49 the insufficient resolutions of sediment samples caused by low deposition rates in many
50 locations, the sampling difficulties and specified locations of ice core and coral samples, they are
51 not sufficient for the investigation in large areas, especially in mid-low latitude terrestrial
52 environment.

53 Tree ring is an excellent time-serial material to monitor past climate changes as well as
54 anthropogenic activities due to its wide distribution, easy access, annual resolution, accurate
55 chronology and environmental sensitivity,¹³ which might preserve the environmental
56 radioactivity information both in pre-nuclear and nuclear age and in different locations.
57 Dendrochemistry based on stable isotopic composition and elements concentrations in annual
58 ring as retrospective proxy data has been successfully used to investigate the past environmental

59 change, such as past temperature and precipitation ($\delta^{18}\text{O}$, $\delta^{13}\text{C}$, etc.),¹³ and anthropogenic release
60 of toxic elements to atmosphere (Pb, Cd, Hg, etc.).¹⁴ A few tentative works on regional
61 radioactive deposition (including sources and transport) have also been reported by
62 determination the concentration of radionuclides, such as ^{40}K , ^{137}Cs and ^{134}Cs .¹⁵ Two
63 investigations on ^{129}I in tree ring samples collected near the West Valley NFRP in USA and the
64 Kalsruhe NFRP in Germany were reported.^{16,17} The variation trend of ^{129}I levels in the ring-
65 porous tree (elm, oak and locast), in which vessels are localized in the outmost growth ring,
66 followed the regional deposition pattern of ^{129}I released from local NFRPs.¹⁶ While, the tree
67 rings of semidiffuse to diffuse-porous wood (cherry and maple), where vessels are disseminated
68 throughout the trunk, showed a less matched ^{129}I pattern to the local NFRP releases.¹⁶ This
69 indicates a critical function of vessels in the iodine cross-ring translocation. However, high
70 values of $^{129}\text{I}/^{127}\text{I}$ atomic ratio up to 3.6×10^{-9} were also measured in pre-nuclear rings from ring-
71 porous tree (elm), indicating a cross-ring translocation of iodine occurred too.¹⁶ It is probably
72 due to the negative hydrostatic pressure in vessels compared to that in adjacent parenchymal
73 cells and tracheid cells.¹⁸ Therefore, coniferous tree might be more suitable for less cross-ring
74 translocation of iodine due to no vessels in this species of tree.

75 The Qinghai-Tibet plateau (QTP) has an average altitude of 4000 m and cold ecosystem with
76 widely distributed permafrost,¹⁹ it is therefore quite sensitive to environment changes.
77 Meanwhile, this region is also important for the climate and ecosystem of a large area in the
78 world because it acts as the largest fresh water reservoir in Asia including over $2 \times 10^{11} \text{ m}^3$ of
79 glacier resource, $3 \times 10^{10} \text{ m}^3$ of annual runoff and 1800 lakes. In 1964 -1980, 22 atmospheric
80 nuclear tests with the total yield of 22.72 Mt of TNT were conducted at Lop Nor NWTs site in
81 Northwest China.²⁰ Due to the prevailing Westerlies at Lop Nor, the released ^{129}I from the

82 atmospheric nuclear weapons tests at this site might be transported to the QTP which is located
83 in the 1100 km downwind area of Lop Nor.

84 This work aims to investigate the sources, transport pathway and transfer of atmospheric
85 iodine in the QTP by determining ^{127}I and ^{129}I in tree rings of spruce. The feasibility using tree
86 rings of spruce to record the temporal variation of iodine isotopes in the atmosphere will be
87 investigated in order to obtain a historic record of ^{129}I and ^{127}I levels in the atmosphere; this is
88 useful for reconstruction of the levels of radioactive fallout and providing fundamental database
89 for regional environmental change research.

90

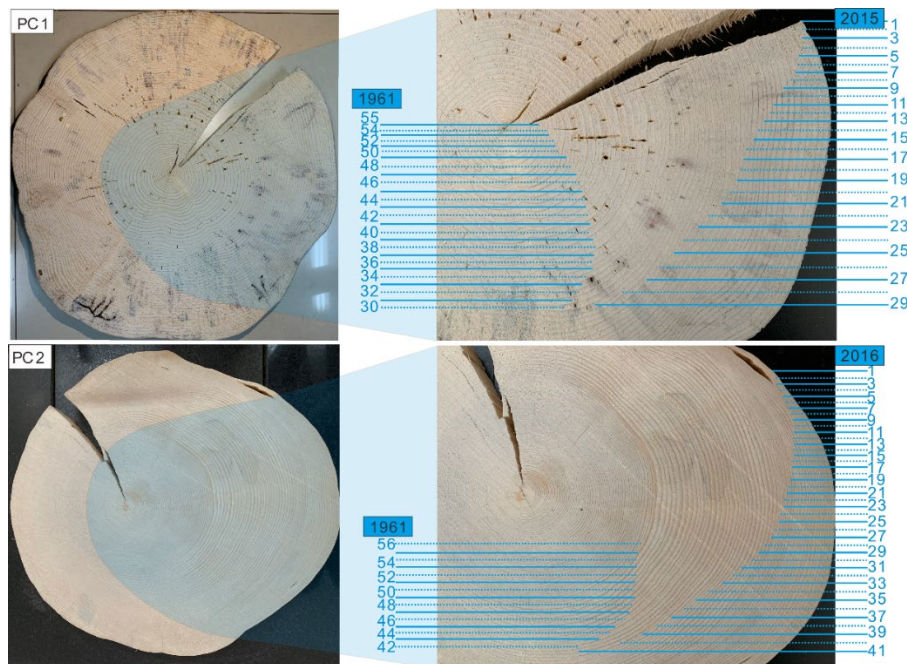
91 **MATERIALS AND METHODS**

92 *Materials and dendrochronology.* Two tree disks of Qinghai spruce PC1 and PC2 were collected
93 from Qunjia (36° 16' 44.04" N, 101° 40' 5.76" E) and Maixiu National Park (35° 16' 26.46" N,
94 101° 55' 1.26" E) in Qinghai province, China, respectively. The sampling sites are located in the
95 northeast edge of the QTP with average altitude over 3000 m and typical plateau continental
96 climate. The Westerly is the dominant wind in this region.¹⁹

97 Qinghai spruce (*Picea crassifolia* Kom.), a coniferous species, is the dominant forest species
98 in this area. Due to banned logging in the virgin forests in China in the past two decades, only
99 the trees that naturally fell down can be sampled. In June 2017, one disk (PC1) was sampled
100 from a spruce tree, which fell down in Dec 2015 in the foot of a slope of 10-20° with low canopy
101 density. Another disk (PC2) was sampled from a spruce, which fell down in Jan 2017 in the
102 middle of a slope of 20° with moderate canopy density. The sampling site of PC2 is located 110

103 km southeast of PC1. A disk of about 5 cm thickness was taken from the trunk of each tree at a
104 height of 30 cm above the ground and transported to the laboratory for analysis.

105 The tree disks were naturally air dried in a cool and ventilated room in Xi'an, China. The
106 surface of the wood disks was polished with sandy papers to easily identify the annual ring by
107 different colors between early and late wood (Fig. 1). No visible multiple rings with abnormal
108 thin width or missing rings with discontinuous boundary were observed in the transection of both
109 disks. Therefore, they were dated by counting rings from outside according to date of fall. The
110 age span is from 1961 to 2015 in PC1, and 1961 to 2016 in PC2 (Fig. 1). An uncertainty of ± 1
111 year for each tree disk was estimated due to the possibility of visual inspection error. The center
112 part of the disk could not be used due to limited massive ring with super thin width. The clearest
113 part with arrayed rings was selected to dissect the annual ring from the outmost layer (Fig. 1).
114 Each dissected sample was dried at 60°C until constant weight, and then cut into small pieces.



115

116 Fig. 1 Wood disks of PC1 tree (up) and PC2 tree (bottom), showing the annual rings

117 *Analytical Methods.* Iodine in the dried tree ring samples was separated using an oxidative
118 combustion method modified from Hou and Wang.²¹ 5 g of dried sample was combusted in a
119 tube furnace (Raddec LTD, Southampton, UK) with a stepwise temperature increasing protocol
120 as shown in Fig S1. Due to the ignition point of about 270 °C in the major part of this type of
121 wood, a slow increase of temperature during 230-350 °C was used to avoid production of a large
122 amount of combustion gases (CO₂, CO, NO_x) in a short time. A second carbonization was
123 implemented by increasing the temperature from 350 to 550 °C in a ramp speed of 2.5 °C /min to
124 combust the remained residues (including rosin with ignition point of 480-500 °C). Afterwards,
125 the temperature was increased to 800 °C and remained for 3 hours to completely decompose the
126 sample. Iodine released during combustion was collected in a bubbler with 30 ml trap solution of
127 0.4 mol/l NaOH-0.05 mol/l NaHSO₃. The detailed method was presented in the supporting
128 information. 1.0 ml of iodine trap solution was diluted with deionized water for measurement of
129 ¹²⁷I using ICP-MS (Agilent 8800 ICP-MS). Cs⁺ was used as internal standard, 0.15 mol/L
130 NH₃·H₂O was used as rinse solution. The detection limit of this method for ¹²⁷I was estimated to
131 be 0.012 ng/ml. Due to large dilution (more than 30 times) of iodine trap solution, the iodine
132 concentrations in some samples from PC2 are close to the detection limit (0.006 µg/g), causing a
133 large measurement uncertainty (> 50%). Therefore, data of these samples are not included for
134 further discussion. After addition of stable iodine carrier (prepared from iodine crystal purchased
135 from Woodward company with ¹²⁹I/¹²⁷I atomic ratio <2×10⁻¹⁴) into the remaining trap solution,
136 iodine (iodide) was precipitated as AgI for determination of ¹²⁹I by a 3 MV Tandem AMS system
137 (HVEE) at Xi'an AMS Center, China. The details of AMS system and measurement method for
138 ¹²⁹I have also been reported elsewhere,²² and briefly described in Supporting Information.
139 ¹²⁹I/¹²⁷I ratios in the procedure blanks prepared using the same procedure as the samples were

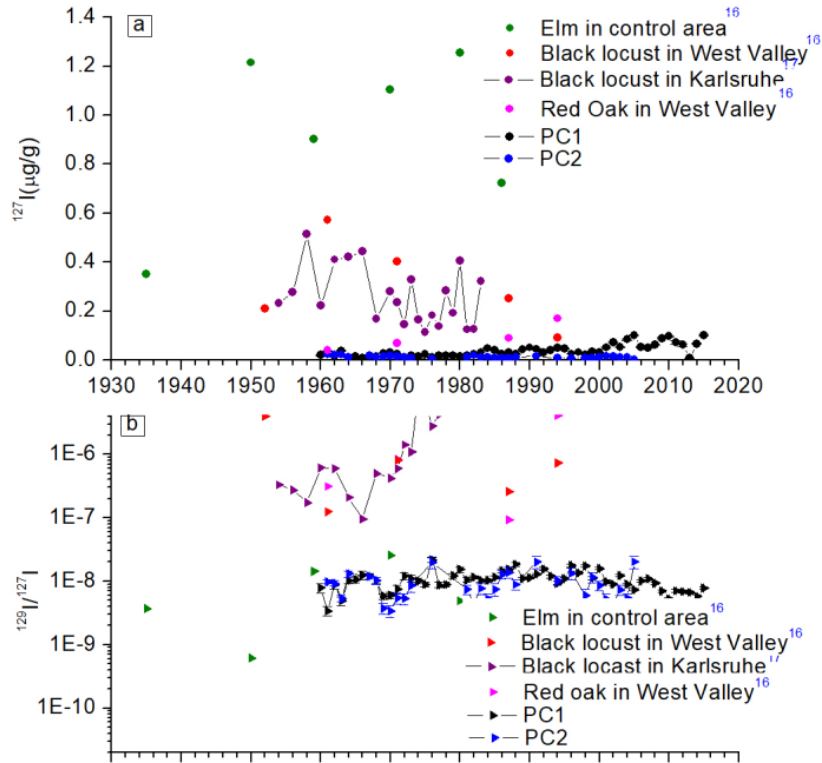
140 measured to be below 2×10^{-13} , which are at least one order of magnitudes lower than that of
141 samples.

142

143 **RESULTS AND DISCUSSION**

144 *¹²⁷I and ¹²⁹I level in the tree rings.* The measured ¹²⁷I concentrations are 0.01-0.10 µg/g with the
145 most data fall into the range of 0.02-0.05 µg/g in tree rings of PC1, and 0.008-0.025 µg/g with
146 the most fall into the range of 0.01-0.02 µg/g in tree rings of PC2 (Fig. 2 a). The higher iodine
147 concentration from PC1 might be attributed to its sampling location, at forest edge with
148 sufficient water, sunlight and fresh air, confirmed by its larger ring width than that of PC2. The
149 iodine concentrations in the two spruce trees are much lower than the reported levels in
150 deciduous trees, such as 0.1-0.6 µg/g in Black locust collected from Karlsruhe, Germany in
151 1954-1983, 0.7-1.2 µg/g in Elm from New York State, USA in 1950-1986 and 0.04-0.09 µg/g in
152 Red Oak from New York State, USA in 1961-1987 (Fig. 2 a).^{16,17} This probably caused by low
153 uptake capacity of iodine from environment in this region with low temperature and associated
154 low growth rate.

155 Significant variations of ¹²⁹I concentrations were observed in two tree rings, i.e. $(0.7-3.5) \times 10^6$
156 atoms/g in PC1 and $(0.5-3) \times 10^6$ atoms/g in PC2 (Fig. S3, Table S1). The over fivefold
157 difference in 55-56 years might be attributed to the varied sources and concentrations of ¹²⁹I in
158 the environment. In addition, the variation might also result from the varied accumulation/uptake
159 rate of iodine into tree rings in different periods. To overcome this problem, the ¹²⁹I/¹²⁷I atomic
160 ratios were applied to represent the level of ¹²⁹I in the tree rings.



161
 162 Fig. 2 Comparison of measured ^{127}I concentrations (a) and $^{129}\text{I}/^{127}\text{I}$ ratios (b) in the tree rings in
 163 this work with the reported values in other locations^{16,17, 23, 24}

164 The $^{129}\text{I}/^{127}\text{I}$ atomic ratios of $(6-15)\times 10^{-9}$ were obtained in the tree ring of PC1 and $(4-20)\times 10^{-9}$
 165 in PC2 (Fig. 2 b), which are more than two orders of magnitude higher than the pre-nuclear level
 166 of $^{129}\text{I}/^{127}\text{I}$ ratios (1.5×10^{-12} for marine system and 2.0×10^{-11} in terrestrial environment),^{5,25}
 167 indicating anthropogenic sources of ^{129}I . However, this level is at least two orders of magnitude
 168 lower than the values reported outside the nuclear fuel reprocessing sites in Germany (10^{-7} - 10^{-5})
 169 and USA (10^{-7} - 10^{-6}), but similar to those observed in the areas without direct influenced by
 170 nuclear activities (10^{-9} - 10^{-8}) (Fig. 2 b).^{16,17} The average ratio of $^{129}\text{I}/^{127}\text{I}$ in the two rings in 2009-
 171 2015 is around 6×10^{-9} , in the same magnitude with the values measured in herbs (4.5×10^{-9})
 172 collected in 2015²³ and surface soils (3×10^{-9}) collected in 2013²⁴ in north China, representing the
 173 level of ^{129}I in this region.

174 *Iodine uptake and integration in the tree rings from atmosphere.* The measured $^{129}\text{I}/^{127}\text{I}$ ratios
175 (average of 6.6×10^{-9}) during 2009-2015 in the rings of PC1 tree are more than two times higher
176 than the reported values in surface soil (average: 3×10^{-9} , collected in 2009-2013) and river water
177 (1.1×10^{-9} , collected in 2016-2017) in nearby locations (Fig. 2).^{24,26} During 1963-1977, the ratios
178 (average of 9.5×10^{-9}) in the rings of both trees are similar to the reported $^{129}\text{I}/^{127}\text{I}$ ratios (average
179 of 9×10^{-9}) in the atmospheric fallout in Tokyo (35 °N) before the operating of Tokai NFRPs (Fig.
180 4a).²⁷ No ^{129}I data in atmospheric sample from the study region was reported. Since the ^{129}I level
181 in atmosphere in the study region (36 °N) should be similar with that in the same latitude region
182 as Tokyo, the result might indicate that iodine uptake from atmosphere is the dominant way
183 entering into the tree rings compared to that from soil system.

184 The Qinghai spruce uptakes inorganic elements and water from soil through root, and
185 translocates it to other parts through the pits on the tracheids cells wall relying on transpiration
186 stream (Fig. S2). This slow process could induce a time lag of months to years.²⁸ Meanwhile,
187 spruce can also uptake the nutrient from atmosphere through foliar absorption, and phloem
188 transport, then to inner xylem through radially aligned ray parenchyma cells (the only radial
189 transport tissue of tree trunk), which is sustainable by photosynthesis energy without much time
190 lag.²⁹

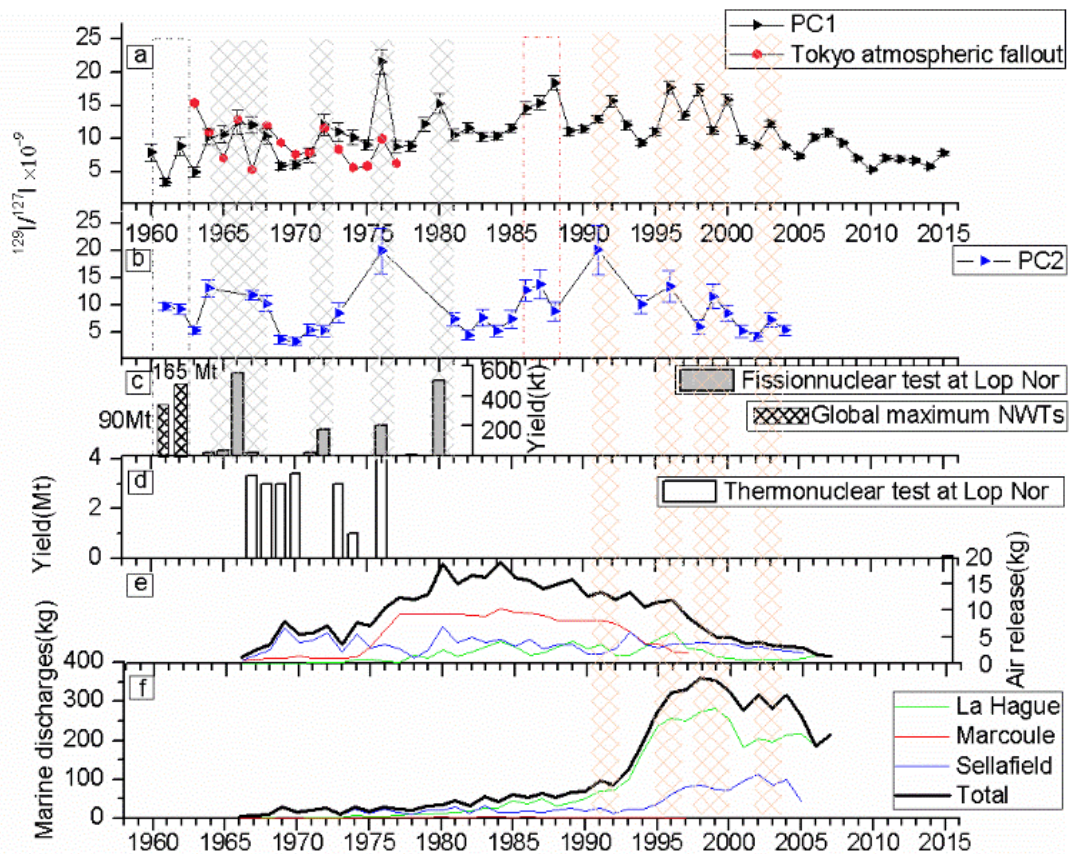
191 Iodine in soil mainly originates from the atmospheric deposition, decomposition of dead
192 plants and animals (absorbed iodine from atmosphere or soil), and weathering of parent material
193 of soil.³⁰ The anthropogenic ^{129}I presents mainly in the upper 50 cm of soil profiles in the
194 background region (far away from any nuclear facilities),³⁰ and the natural $^{129}\text{I}/^{127}\text{I}$ ratios in the
195 deep soil ($<10^{-11}$) are 2-3 orders of magnitude lower than the present environmental level (e.g.
196 atmosphere, surface soil, etc.).²⁵ Considering the deep root of spruce ($>>50$ cm), lower $^{129}\text{I}/^{127}\text{I}$

197 ratios observed in the surface soil in this region compared to that in the tree ring, as well as the
198 similar $^{129}\text{I}/^{127}\text{I}$ ratios of the tree rings with that in atmospheric fallout in Japan, iodine in the
199 investigated tree rings should be dominantly taken from atmosphere. The similar pattern of
200 higher $^{129}\text{I}/^{127}\text{I}$ ratios in precipitation (3.8×10^{-9}) than that in surface soil (1.9×10^{-9}) was also
201 reported in Xi'an.³¹ Due to the non-essential element for trees, iodine was also demonstrated to
202 be hardly translocated to the aboveground compartments from the tree root system.²⁹

203 In atmosphere, iodine presents mainly in gaseous form and partly associated with aerosol.^{32,33}
204 Gaseous iodine can be trapped directly through stomata in the tree leaves. Aerosol deposited on
205 tree leaves might be adhered on the surface through wax on the spruce needles, and the
206 associated iodine can be leached out by water vapor. Then soluble iodine can be taken up to the
207 tree leaves through hydrophilic holes on leaf's surface and/or active absorption by
208 plasmodesmata.³⁴ The absorbed iodine is translocated through phloem, ray parenchyma cells and
209 then fixed in xylem. The Fukushima derived ^{129}I was observed to be well recorded in *Japanese*
210 *cedar* (coniferous species) through atmosphere absorption.³⁵ Much higher ^{129}I concentration was
211 measured in litter than in surrounding soil collected in nearby area of a NFRP, implying a more
212 direct uptake way of iodine in tree/vegetation from atmosphere by foliage.¹⁷

213 The translocation pathway of the atmospheric uptake iodine into the xylem relies on the only
214 radial tissue (ray parenchyma cells) and the pits on longitudinal tracheid cell walls (Fig. S2). The
215 ray parenchyma cells, is alive only in sapwood (usually the out most 10-12 rings) but dead in
216 heartwood.³⁶ A considerable amount of radial moving of water solution in alive ray parenchyma
217 cells was detected based on fluorescein dyes.¹⁸ However the migration depth was limited only in
218 the outmost ring of mature xylem from the anatomical observations by scanning electron
219 microscope.¹⁸ A similar low crossing rings movement of water soluble fluorine (similar

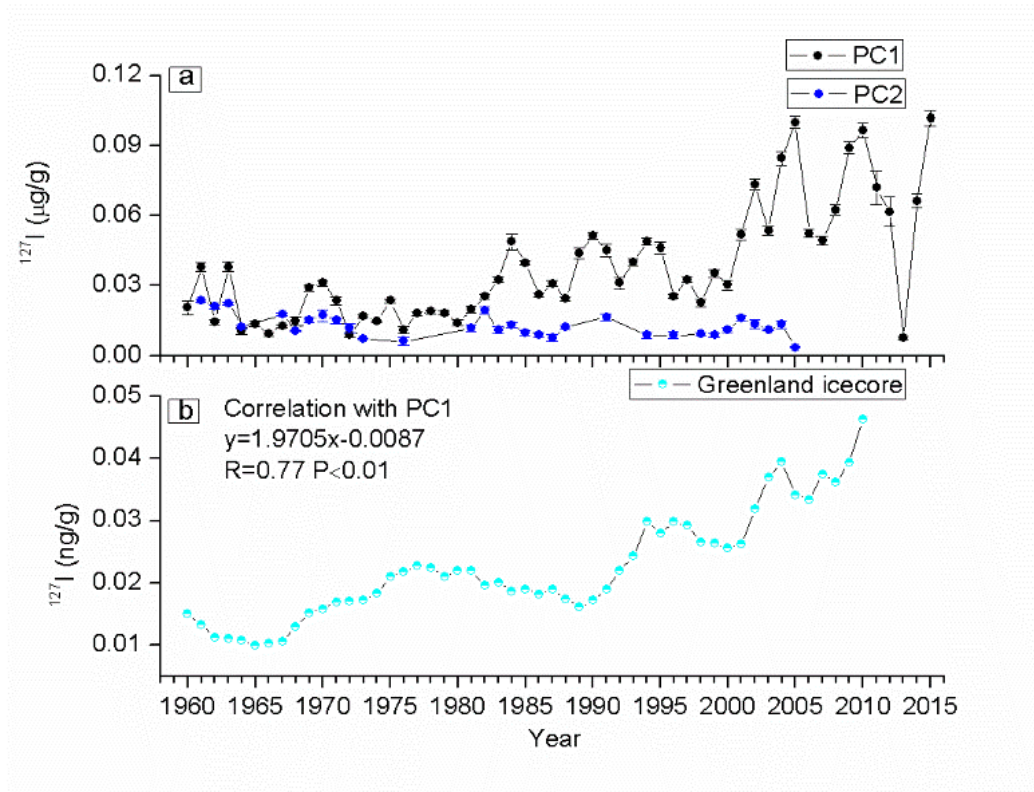
220 chemistry with iodine) was also reported in Norway spruce.³⁷ The pits in longitudinal tracheid
 221 cells are usually less developed, both the size and quantity, from late wood than that from early
 222 wood, which will primarily limit iodine moving across one single growth ring. The water
 223 transport by tracheid cells was only observed in early wood, but not in late wood based on single
 224 growing spruce ring.³⁷ Combined with the fluctuated variation of the observed $^{129}\text{I}/^{127}\text{I}$ ratios
 225 over rings in both trees (Figure. 3a and b) instead of monotonous gradient distributions, it
 226 indicates that the crossing rings translocation of iodine hardly happens in the selected Qinghai
 227 spruce.



228
 229 Fig. 3 Temporal variation of the measured $^{129}\text{I}/^{127}\text{I}$ ratios in the tree rings from two sites in the
 230 QTP (a), in comparison with the reported variation of $^{129}\text{I}/^{127}\text{I}$ in atmospheric fallout from
 231 Tokyo (b)²⁷, yield of fission NWTs (c), yield of thermonuclear weapons tests at Lop Nor

232 (d) ²⁰, air releases of ¹²⁹I from major NFRPs (e) and marine discharges of ¹²⁹I from
233 NFRPs (f).³³

234 *Historic records of atmospheric iodine level.* ¹²⁷I concentrations in the tree rings of PC1 (Fig. 4a)
235 were 0.010-0.033 µg/g with an average of 0.020 µg/g in 1961-1983, and increase to 0.023-0.051
236 µg/g with an average of 0.039 µg/g in 1984-2001, then to 0.049-0.100 with an average of 0.069
237 µg/g in 2001-2016. A threefold increase was observed, but no such variation in PC2 (Fig. 4a).
238 This increased iodine concentrations might reflect the increased iodine concentrations in
239 atmosphere based on the inferred atmospheric absorption pathway. A similar three folds
240 elevation of atmospheric iodine has been observed in Alpine ice core,⁴ and Greenland ice core ³
241 from 1950-2000s. Significant correlation of ¹²⁷I concentrations in the tree rings with that in
242 Greenland ice core³ (directly deposition from atmosphere) (R=0.77, P<0.01) are observed (Fig.
243 4b). However, no such kind of correlation was found in PC2. The lack of partial data in PC2
244 or/and the sampling site located in the middle of forest with higher canopy density than that in
245 PC1 and lower environmental sensitivity might attribute to this phenomenon.³⁸ Although the
246 uptake capacity of iodine through the foliar absorbing way can be affected by water condition,
247 sunlight, temperature, etc., a less variation of temperature (<1°C of the annual average
248 temperature), fluctuating variation of annual precipitation (from the nearest Xining weather
249 station), and almost steady sunlight condition were reported in the past 50-60 years in the
250 studied time scale,³⁹ excluded effect of these parameters on the uptake of iodine into the tree
251 region in this location.



252

253 Fig. 4 Variation of iodine (^{127}I) concentration in PC1 and PC2 tree (a), in comparison with the
 254 temporal variation of iodine concentrations in ice core in Greenland³

255 Iodine in atmosphere might originate from oceanic emissions of gaseous iodine (through
 256 biological, chemical and photochemical process), terrestrial emissions of gaseous iodine from
 257 salt marches, rice fields, peatland and forest system, and combustion of fossil fuel and biomass,
 258 of which the oceanic emission dominates.^{1,3,4} The increased atmospheric iodine level might be
 259 attributed to the increased releases from these processes. The oceanic emission of molecular
 260 iodine (I_2) was observed to increase with the tropospheric ozone (O_3) content,¹ which increased
 261 by a factor of two from the 1950s to early 1990s due to the elevated global combustion of fossil
 262 fuel.^{40,41} The oceanic emission iodine was reported to be enhanced by the sub-ice phytoplankton
 263 production that associated with the recent thinning of sea ice.³ Meanwhile, the increased

264 consumption of fossil fuels (from 1000 TWh/y in 1980s to 3200 TWh/y in 2000s) in the past
265 decades could also directly contribute to the increased iodine concentration in the atmosphere,
266 which was estimated to be 5000 tons/y in 2005.^{42, 43}

267 *Records of human nuclear activities in the tree rings.* The distribution of $^{129}\text{I}/^{127}\text{I}$ atomic ratios
268 (Fig. 3a and b) in the two tree rings show similar variation trend, e.g. the $^{129}\text{I}/^{127}\text{I}$ peaks in 1962,
269 1964-1968, 1976, 1996 and 2003 occurred in both tree rings, as well as the peaks in 1972/1973,
270 (1986-1988)/(1986-1987), 1992/1991, 1998 and 2000/1999 occurred in PC1/PC2 respectively.
271 The one-year discrepancy between the records in two tree rings could be caused by the
272 uncertainty of dating (± 1) from counting rings. In addition to that, due to the lack of data in 1980
273 in PC2 rings compared to an obvious peak in 1980 from PC1 rings, and a separate high values
274 period of 2006-2008 in PC1 rings, might be attributed to the different sampling locations and/or
275 uncertainty of dating results (± 1 year) from counting rings.

276 The similar peaks in the two tree rings should be attributed to the peak values of ^{129}I occurred
277 in atmosphere during these years, resulting from the anthropogenic releases. Fig. 3 shows the
278 variation of $^{129}\text{I}/^{127}\text{I}$ ratios in two tree rings in comparison with that in atmospheric fallout
279 records in Tokyo (Fig. 3a and b), the time distribution of explosion yields of atmospheric NWTs
280 (Fig. 3c and d), and the annual discharges (air and marine) of ^{129}I from the three European
281 NFRPs which accounts for the most of ^{129}I inventory in current environment (Fig. 3e and f).

282 Atmospheric nuclear weapons tests. Several peaks of $^{129}\text{I}/^{127}\text{I}$ atomic ratios in 1962, 1964-1968,
283 1972, 1976 and 1980 were observed in the tree rings of PC1, and in 1961-1962, 1964-1968 and
284 1976 in the rings of PC2. The atmospheric nuclear weapon tests are the only source of ^{129}I during
285 this period since the release amount from NFRPs were negligible.²⁰

286 The twofold increased $^{129}\text{I}/^{127}\text{I}$ ratios (8.8×10^{-9}) in 1962 compared to the value of $(3-4) \times 10^{-9}$
287 in 1961 and 1963 was observed in tree rings of PC1, and 9×10^9 in 1961-1962 compared to 5×10^9
288 in 1963 in PC2 rings, corresponding with the date of the largest numbers of atmospheric NWTs
289 in 1961-1962. The observed value in the tree rings of 1961-1962 (average: 9×10^9) agrees with
290 the value recorded in atmospheric fallout samples in 1963 from Tokyo (15.5×10^9).²⁷ This signal
291 was widely detected by peaks of $^{129}\text{I}/^{127}\text{I}$ ratio, ^{137}Cs and $^{239,240}\text{Pu}$ activities in north China.^{7,44}
292 The 1-2 years lag among these records could be attributed to the hysteresis effect of samples
293 or/and the dating uncertainty (± 1 year).

294 A broad peak of $^{129}\text{I}/^{127}\text{I}$ ratios corresponding to 1964-1968 was observed in both tree rings,
295 which matches well with several high fission yield tests at Lop Nor (Fig. 3c), such as the first
296 one in 1964 (20 kt) and the second one in 1965 (40 kt). The highest value of 12×10^9 in 1966 in
297 PC1 rings agrees well with the boosted fission tests carried in 1966 with fission yield of 250 kt of
298 TNT, and the similar high $^{129}\text{I}/^{127}\text{I}$ ratio (12×10^9) was also recorded in atmospheric fallout
299 samples in 1966 collected from Tokyo.²⁷ The constant high ^{129}I level in both trees in 1967-1968,
300 as well as the high value in the atmospheric fallout in Tokyo in 1968, should be attributed to a
301 test of fission weapon in 1967 at Lop Nor and the first two Chinese thermonuclear weapons tests
302 in 1967 and 1968, where a detonator with high ^{235}U fuel load might be applied, causing releases
303 of fission products including ^{129}I .

304 The radioactive substances from atmospheric NWTs were injected into different height of
305 atmosphere depending on the total explosion yield, the height of burst, and the meteorological
306 condition after the detonation.²⁰ The radioactive substances from fission weapons with relative
307 lower yields and some part from thermonuclear weapons were mainly injected into troposphere
308 to disperse regionally.²⁰ The sampling sites in northeast QTP are located about 1100 km

309 southeast of Lop Nor. The dominant Westerlies in the troposphere in the Lop Nor region can
310 transport these radioactive substances (including ^{129}I) to the sampling sites in several days and
311 produce $^{129}\text{I}/^{127}\text{I}$ ratio peaks in the tree rings. The simulated forward trajectories of air masses by
312 the HYSPLIT model (Fig. S4) confirmed that the air masses in the troposphere at the Lop Nor
313 after the tests on 16th Oct. 1964, 14th May 1965, 28th Dec. 1966, 17th Jul. 1967, and 28th Dec.
314 1968 reached to the sampling region in a few days.⁴⁵

315 One $^{129}\text{I}/^{127}\text{I}$ ratio peak, observed in 1972 in PC1 rings, is in accord with the high fission yield
316 of 170 kt of TNT from a fizzled thermonuclear test conducted on 18th Mar. 1972 at Lop Nor. No
317 significant peak of $^{129}\text{I}/^{127}\text{I}$ ratio was observed in 1972 but a high value in 1973 (8.5×10^{-9}) in
318 PC2, which could be due to the ± 1 year's uncertainty of dating. A similar peak was also
319 measured in atmospheric fallout samples in 1972 collected from Tokyo (11.5×10^9) (Fig. 3a).²⁷
320 The highest value of $^{129}\text{I}/^{127}\text{I}$ ratios of 20×10^{-9} was observed in 1976 in both tree rings that
321 matches very well with the date of the fizzled thermonuclear test with a high fission yield of 200
322 kt of TNT on 26th Sep. 1976 at Lop Nor, as well as a similar peak in atmospheric fallout in
323 Tokyo.²⁷ A peak value of $^{129}\text{I}/^{127}\text{I}$ ratios (15.3×10^9) was observed in 1980 in PC1 rings in
324 consistent with the time of the last atmospheric test at Lop Nor. The forward trajectory analysis
325 of air mass also confirmed the stratospheric air masses at the Lop Nor after the tests on 18th Mar.
326 1972, 26th Sep. 1976, and 16th Oct. 1980 arrived in the sampling region in a few days (Fig. S4)

327 No significantly high ^{129}I signals were observed after 5 high yield thermonuclear tests
328 conducted on 29th Sep. 1969 (3 Mt), 14th Oct. 1970 (3.4 Mt), 27th Jun. 1973 (3 Mt), 17th Jun.
329 1974 (1 Mt) and 17th Nov. 1976 (4 Mt) (Fig. 3d), reflecting less ^{129}I release due to the less fission
330 fuel loaded as detonator.

331 Releases from nuclear accidents. A peak of $^{129}\text{I}/^{127}\text{I}$ ratios covers 3 years in 1986-1988 ((14.6-
332 18.4) $\times 10^9$) in PC1, and 2 years in 1986-1987 ((12.7-13.8) $\times 10^9$) in PC2 were observed. Since
333 atmospheric NWTs have already been ceased from 1980, and the almost steady discharges of ^{129}I
334 from the main NFRPs (air: 13-14 kg/y; marine: 70 kg/y), this might be attributed to the
335 Chernobyl accident on 26th April 1986 with 1.3-6 kg ^{129}I released to the environment.³³ The
336 Chernobyl accident derived radioactive fallout had dispersed to north China through the
337 Westerlies, and the level decreased from northwest towards east and south.⁴⁶ The total β activity
338 in atmospheric fallout collected in Urumchi (1400 km in the northwest of sampling sites, 43° N),
339 and the short lived radioactive ^{131}I activity in milk was observed to elevate over 50 times
340 compared to the background value.^{46,47} A 15-times elevation of the total β activity was also
341 measured in atmospheric fallout in Xi'an (600 km in the east of sampling sites, 33° N).⁴⁷
342 Although no direct monitor data of radioactivity after the Chernobyl accident is available in the
343 sampling site, it should receive the Chernobyl derived ^{129}I because the sampling site is located
344 between Xi'an and Urumchi. The Chernobyl derived $^{129}\text{I}/^{127}\text{I}$ peak was even observed in
345 sediment samples from Jiaozhou Bay in the similar latitude but 1600 km east to the study area.⁷
346 A broad ^{129}I peaks in both tree ring profiles (PC1: 3 years; PC2: 2 years) might be contributed to
347 the re-emission of the deposited ^{129}I in the high contaminated soil to atmosphere in the following
348 2-3 years.

349 No significant increased $^{129}\text{I}/^{127}\text{I}$ value was observed in 2011 (7.1×10^9) compared to 6.9×10^9
350 in 2012 and 5.2×10^9 in 2010 in PC1 rings, indicting an insignificant contribution from the
351 Fukushima accident with about 1.2 kg ^{129}I releases (including 0.35 kg direct marine discharge).⁷
352 The atmospheric releases from Fukushima accident mainly dispersed eastwards and deposited in
353 the North Pacific Ocean, and the marine discharges including ^{129}I were mainly transported

354 eastwards by North Pacific Current.⁴⁸ Although some radionuclides (mainly ¹³¹I, ¹³⁷Cs and ¹³⁴Cs)
355 in aerosol samples collected in North China after Fukushima were measurable, but the level is
356 much lower compared to those in North America and Europe, and at least two orders of
357 magnitudes lower than that from Chernobyl.^{49,50,51} Therefore, the contribution to the study area is
358 negligible.

359 Releases from nuclear fuel reprocessing plants. A few peaks of ¹²⁹I/¹²⁷I ratios were observed
360 since 1991 in the rings of both trees, i.e. 1992 (PC1)/1991 (PC2), 1996 (PC1 and PC2), 1998 and
361 2000 (PC1)/1999 (PC2) and 2003 (PC1 and PC2) (Fig. 3a and b). Since the atmospheric NWTs
362 ceased in 1980, no reported nearby nuclear facilities and nuclear accidents can release ¹²⁹I to the
363 sampling region. The most possible source of ¹²⁹I during this period should be the releases from
364 NFRPs, which dominate the ¹²⁹I inventory in the present environment.³³ Although the
365 reprocessing plants have been in operation in USA, Russia, Japan, China, Germany, France and
366 UK, the European reprocessing plants in Marcoule (1959-1997), La Hague (1966-), and
367 Sellafield (1951-) are the most important ones due to their high capacities and large scales in
368 reprocessing operation. The contribution from two Chinese reprocessing plants in Guangyuan
369 (1975-1991) and Jiuquan (1968-1984) was insignificant due to the small capacity and ¹²⁹I release
370 compared to the European ones.²⁰ The investigation of ¹²⁹I distribution in surface soil from a
371 large area of China did not show any unexpected increase level, except the local region of these
372 two NFRPs (<100 km).⁵² The contribution from Tokai NFRPs (1977-2005) in Japan should be
373 negligible because of the small volume of ¹²⁹I release (1 kg), the far distance, and non-major
374 direction of wind.²⁰

375 The total atmospheric release of ¹²⁹I from the three European NFRPs gradually increased to
376 10 kg/y in 1976 from lower than 5 kg /y in late 1960s, and then kept at a relative constant high

377 level of about 15 kg /y until 1996. Afterwards, it gradually decreased to a quite low value of 1.4
378 kg/y in 2007 due to the shutdown of NFRP at Marcoule in 1997 and the updated system in other
379 reprocessing plants for capture of gaseous radioiodine (Fig. 3e).³³ The high value in 1980 (18 kg)
380 compared to that in 1979 (13 kg) might add a small background value on the peak produced by
381 the last Chinese NWT. The marine discharges, mainly from the two European reprocessing
382 plants at La Hague (France) and Sellafield (UK), gradually increased to 65 kg/y in 1980s from
383 less than 40 kg/y before that, and significantly increased after 1990 and keep at a high value of
384 250 kg/y (Fig. 3f).

385 The ¹²⁹I peak observed in both tree rings in 1991/1992 matches well with the first increased
386 total marine discharges (to 100 kg/y in 1991 from 70 kg/y in 1990), when air discharges of 13 kg
387 were steady. The peak observed in 1996 matches with the most drastically elevated marine
388 discharges up to 320 kg/y from below 200 kg/y in 1995, under the almost steady air discharges
389 of (9-12) kg/y. The peaks observed in 1998-2000 in the two tree rings agree with the first peak of
390 marine discharges of 350 kg/y in 1998-1999, while the air discharges continuously reduced by
391 half (1997: 9 kg; 1999: 5 kg). The peak in 2003 matched well with the high value of 360 kg/y of
392 marine discharges in 2002 compared to the value of 280 kg/y in 2001 and 2003, under the almost
393 steady air discharges of 4 kg/y (Fig. 3e and f).

394 Some exceptional events were not recorded in tree rings, such as the elevation of total air
395 discharges from 16 kg/y in 1983 to 19 kg/y in 1984, and the three-time elevation of total marine
396 discharges from 100 kg in 1991/1992 to 325 kg in 1996. The small increment could be
397 responsible for the former one. The decreased air discharges from Marcoule NFRPs from 8 kg/y
398 in 1991/1992 to 2 kg/y in 1996 could explain the later one due to the closer latitude of 43 °N
399 compared to that of La Hague (49° N) and Sellafield (54° N).

400 The marine discharges of ^{129}I can be re-emitted to the atmosphere in gaseous form confirmed
401 by the similar high $^{129}\text{I}/^{127}\text{I}$ ratios observed in aerosols and rainwater samples collected in the
402 North Europe (Denmark, Germany and Sweden) and the contaminated seawater samples ($^{129}\text{I}/^{127}\text{I}$
403 = 10^{-8} - 10^{-6}).^{32,53} The re-emitted ^{129}I can enter into lower troposphere, and to higher altitude by
404 intensive vertical motions, then further transport eastwards through the Westerlies (around 1500
405 m-12000 m, mainly in 35°N - 65°N) to East Asia. The European NFRPs derived ^{129}I signal has
406 been observed in sediment,^{6,7} precipitation,⁵⁴ and ground water²⁶ in Westerly area of north China
407 ($> 33^\circ\text{N}$). The ^{129}I was finally taken up by tree leaves and recorded as $^{129}\text{I}/^{127}\text{I}$ ratio peaks in both
408 tree rings within 1 year in consideration of the long-distance transport.

409 Above all, the sources, transport pathway and transfer process of atmospheric iodine in the
410 northeast part of the QTP were well traced. The terrestrial iodine from northwest upwind area
411 (traced by ^{129}I released from NWTs at Lop Nor and from Chernobyl Accident), and marine
412 iodine from the mid-high latitude of Atlantic Sea (traced by ^{129}I released from NFRPs at
413 Sellafield, La Hague and Marcoule) can be transported to the studied area through the Westerlies,
414 which contribute significantly for the iodine in atmosphere and then ecosystem.

415 **SUPPORTING INFORMATION**

416 The detailed chemical separation procedure, preparation and measurement of ^{127}I and ^{129}I , the
417 tissues, the microscopic structures of selected wood species are presented; The analytical results
418 of ^{129}I and ^{127}I concentration in two tree rings (Table S1), protocol of combustion for iodine
419 separation from wood (Fig. S1), diagram of tree rings and microstructure of nonporous and
420 porous tree (Fig. S2), temporal variations of ^{129}I concentrations in PC1 and PC2 (Fig. S3), and
421 simulated forward trajectories of air mass after the major Chinese atmospheric nuclear weapons
422 tests (Fig. S4) are included.

423

424 **ACKNOWLEDGEMENTS**

425 This work was supported by the Ministry of Science and Technology of China (No.
426 2015FY110800), the National Natural Science Foundation of China (No. 11875261, 91643206,
427 11605206, 41603125), Chinese Academy of Sciences (132B61KYSB20180003), National
428 Research Program for Key Issues in Air Pollution Control (DQGG0105-02). AMS measurement
429 of ¹²⁹I was performed by Dr. Qi Liu in the Xi'an AMS Center. X. Zhao thanks Xuhong Jiang,
430 Xiaohu Xiong, Jing Li and Miao Fang from Institute of Earth Environment for their helps in the
431 sampling and sample preparation and Dr. Jixin Qiao from the Technical University of Denmark
432 for her constructive suggestions in the manuscript preparation. The authors gratefully
433 acknowledge the NOAA Air Resources Laboratory (ARL) for the provision of the HYSPLIT
434 transport and dispersion model (<http://www.ready.noaa.gov>) used in this publication.

435

436 **References**

- 437 (1) Carpenter, L. C.; MacDonald, S. M.; Shaw, M. D.; Kumar, R.; Saunders, R. W.; Parthipan, R.;
438 Wilson, J.; Plane, L. M. Atmospheric iodine levels influenced by sea surface emissions of inorganic
439 iodine. *Nature Geoscience*. **2013**, *6*(2), 108-111; DOI 10.1038/ngeo1687.
- 440 (2) Gantt, B.; Sarwar, G.; Xing, J.; Simon, H.; Schwede, D.; Hutzell, W. T.; Mathur, R.; Saiz-Lopez, A.
441 The impact of iodide-mediated ozone deposition and halogen chemistry on surface ozone
442 concentrations across the continental United States. *Environ. Sci. Technol.* **2017**, *51*(3), 1458-1466;
443 DOI 10.1021/acs.est.6b03556.
- 444 (3) Cuevas, C.; Maffezzoli, N.; Corella, J.; Spolaor, A.; Vallelonga, P.; Kjer, H. A.; Simonsen, M.;
445 Winstrup, M.; Vinther, B.; Horvat, C.; Fernandez, R. P.; Kinnison, D.; Lamarque, J.; Barbante, C.;

- 446 Saiz-Lopez, A. Rapid increase in atmospheric iodine levels in the North Atlantic since the mid-20th
447 century. *Nature Communications*. **2018**, 9(1), 1452-1458; DOI 10.1038/s41467-018-03756-1.
- 448 (4) Legrand, M.; McConnell, J. R.; Preunkert, S.; Arienzo, M.; Chellman, N.; Gleason, K.; Sherwen, T.;
449 Evans, M.; Carpenter, L. J. Alpine ice evidence of a three-fold increase in atmospheric iodine
450 deposition since 1950 in Europe due to increasing oceanic emissions. *Proceedings of the National
451 Academy of Sciences*. **2018**, 115(48), 12136-12141; DOI 10.1073/pnas.1809867115.
- 452 (5) Moran, J. E.; Fehn, U.; Teng, R. T. D. Variations in $^{129}\text{I}/^{127}\text{I}$ ratios in recent marine sediments:
453 evidence for a fossil organic component. *Chemical Geology*. **1998**, 152(1-2), 193-203; DOI
454 10.1016/S0009-2541(98)00106-5.
- 455 (6) Zhao, X.; Hou, X.; Du, J.; Fan, Y. Anthropogenic ^{129}I in the sediment cores in the East China Sea:
456 Sources and transport pathways. *Environmental Pollution*. **2019**, 245, 443-452; DOI
457 10.1016/j.envpol.2018.11.018.
- 458 (7) Fan, Y.; Hou, X.; Zhou, W.; Liu, G. ^{129}I record of nuclear activities in marine sediment core from
459 Jiaozhou Bay in China. *Journal of Environmental Radioactivity*. **2016**, 154, 15-24; DOI
460 10.1016/j.jenvrad.2016.01.008.
- 461 (8) Bautista, Vii A. T.; Miyake, Y.; Matsuzaki, H.; Lizuka, Y.; Horiuchi, K. High-resolution ^{129}I bomb
462 peak profile in an ice core from SE-Dome site, Greenland. *Journal of Environmental Radioactivity*.
463 **2018**, 184-185, 14-21; DOI 10.1016/j.jenvrad.2017.12.015.
- 464 (9) Biddulph, D. L.; Beck, J. W.; Burr, G. S.; Donahue, D. J. Two 60-year records of ^{129}I from coral
465 skeletons in the South Pacific Ocean. *Radioactivity in the Environment*. **2006**, 8, 592-598; DOI
466 10.1016/S1569-4860(05)08047-2.
- 467 (10) Bautista, Vii A. T.; Matsuzaki, H.; Siringan, F. P. Historical record of nuclear activities from ^{129}I
468 in corals from the northern hemisphere (Philippines). *Journal of Environmental Radioactivity*. **2016**,
469 164, 174-181; DOI 10.1016/j.jenvrad.2016.07.022.
- 470 (11) Chang, C. C.; Burr, G. S.; Jull, A. J. T.; Russell, J. L.; Biddulph, D.; White, L.; Prouty, N. G.;
471 Chen, Y.; Shen, C.; Zhou, W.; Lam, D. D. Reconstructing surface ocean circulation with ^{129}I time

- 472 series records from corals. *Journal of Environmental Radioactivity*. **2016**, 165, 144-150; DOI
473 10.1016/j.jenvrad.2016.09.016.
- 474 (12) Prouty, N. G.; Roark, E. B.; Mohon, L. M.; Chang, C. C. Uptake and distribution of organo-
475 iodine in deep-sea corals. *Journal of Environmental Radioactivity*. **2018**, 187, 122-132;
476 10.1016/j.jenvrad.2018.01.003.
- 477 (13) Trevor, J. P.; Michael, F. P.; Steven, V. K.; Thomas, W. D. Climatic signals in $\delta^{13}\text{C}$ and $\delta^{18}\text{O}$ of
478 tree-rings from White Spruce in the Mackenzie Delta Region, Northern Canada. *Arctic, Antarctic,
479 and Alpine Research*. **2009**, 41(4), 479-505; DOI 10.1657/1938-4246-41.4.497.
- 480 (14) Watmough, S. A. Monitoring historical changes in soil and atmospheric trace metal levels by
481 dendrochemical analysis. *Environmental Pollution*. **1999**, 106(3), 391-403; DOI 10.1016/S0269-
482 7491(99)00102-5.
- 483 (15) Haas, G.; Schupfner, R.; Müller, A. Radionuclide uptake and long term behavior of ^{137}Cs , ^{134}Cs
484 and ^{40}K in tree rings of spruce. *Journal of Radioanalytical & Nuclear Chemistry*. **1995**, 194(2), 277-
485 282; DOI 10.1007/BF02038424.
- 486 (16) Rao, U.; Fehn, U.; Muramatsu, Y.; McNeil, H.; Sharma, P.; Elmore, D. Tracing the history of
487 nuclear releases: determination of ^{129}I in tree rings. *Environmental Science & Technology*. **2002**,
488 36(6), 1271-1275; DOI 10.1021/es011045i.
- 489 (17) Hauschild, J. and Aumann, D. C. Iodine-129 and natural iodine in tree rings in the vicinity of a
490 small nuclear fuels reprocessing plant. *Die Naturwissenschaften*. **1995**, 72(5), 270-272; DOI
491 10.1007/BF00448689.
- 492 (18) Sebastian, P.; Justine, R.; Tjoelker, M.; Salih, A. Phloem as capacitor: Radial transfer of water
493 into xylem of tree stems occurs via symplastic transport in ray parenchyma. *Plant Physiology*. **2015**,
494 167(3), 963-971; DOI 10.1104/pp.114.254581.
- 495 (19) Wang, G.; Li, Y.; Wu, Q.; Wang, Y. Impacts of permafrost changes on alpine ecosystem in
496 Qinghai-Tibet Plateau. *SCIENCE IN CHINA SERIES D-EARTH SCIENCES*. **2006**, 49(11), 1156-
497 1169; DOI 10.1007/s11430-006-1156-0.

- 498 (20) *UNSCEAR, 2000: Sources, Effects and Risk of Ionizing Radiation. UNSCEAR 2000 Report to the*
499 *General Assembly, Annex C: Exposures from Man-made Sources of Radiation*; United Nations
500 Scientific Committee on the Effect of Atomic Radiation: New York, 2000;
501 www.unscear.org/docs/publications/2000/UNSCEAR_2000_Annex-C-CORR.pdf.
- 502 (21) Hou, X. and Wang, Y. Determination of ultra-low level ^{129}I in vegetation using pyrolysis for
503 iodine separation and accelerator mass spectrometry measurement. *Journal of Analytical Atomic*
504 *Spectrometry*. **2016**, 31(6), 1298-1310; DOI 10.1039/C6JA00029K.
- 505 (22) Hou, X.; Zhou, W.; Chen, N.; Zhang, L.; Liu, Q.; Fan, Y.; Liang, W.; Fu, Y. Determination of
506 ultralow level $^{129}\text{I}/^{127}\text{I}$ in natural samples by separation of microgram carrier free Iodine and
507 Accelerator Mass Spectrometry detection. *Analytical Chemistry*. **2010**, 82, 7713-7721; DOI
508 10.1021/ac101558k.
- 509 (23) Wang, Y. Investigation of ^{129}I in vegetation samples from Northwest of China. M.S. Dissertation,
510 Chinese Academy of Sciences (Institute of Earth Environment Science), Beijing, 2016.
- 511 (24) Zhang, D. Iodine and Plutonium isotope distribution and tracer study in Northern China. Ph.D.
512 Dissertation, Chinese Academy of Sciences (Institute of Earth Environment Science), Beijing, 2018.
- 513 (25) Fan, Y.; Zhou, W.; Hou, X. Pre-nuclear level of ^{129}I in Chinese Loess-Paleosol sections: a search
514 for the natural ^{129}I level for dating in terrestrial environments. *Geochimica Et Cosmochimica Acta*.
515 **2018**, 231, 64-72; DOI 10.1016/j.gca.2018.04.014.
- 516 (26) Chen, N. Analysis method of iodine isotope in water samples and its application in environmental
517 tracing. Ph.D. Dissertation, Chinese Academy of Sciences (Institute of Earth Environment Science),
518 Beijing, 2018.
- 519 (27) Toyama, C.; Muramatsu, Y.; Igarashi, Y.; Aoyama, M.; Matsuzaki, H. Atmospheric fallout of ^{129}I
520 in Japan before the Fukushima accident: regional and global contributions (1963-2005).
521 *Environmental Science & Technology*. **2013**, 47, 8383-8390; DOI 10.1021/es401596z.

- 522 (28) Roulrier, M.; Bueno, M.; Thiry, Y.; Coppin, F.; Redon, P.; Hecho, I. L.; Pannier, F. Iodine
523 distribution and cycling in a beech (*Fagus sylvatica*) temperate forest. *Science of the Total*
524 *Environment*. **2018**, 645, 431-440; DOI 10.1016/j.scitotenv.201807.039.
- 525 (29) Momoshima, N. and Bondietti, E. A. Cation binding in wood: applications to understanding
526 historical changes in divalent cation availability to red spruce. *Canadian Journal of Forest Research*.
527 **1990**, 20(12), 1840-1849; DOI 10.1139/x90-247.
- 528 (30) Luo, M.; Hou, X.; Zhou, W.; He, C.; Chen, N.; Liu, Q.; Zhang, L. Speciation and migration of
529 ¹²⁹I in soil profiles. *Journal of Environmental Radioactivity*. **2012**, 118, 30-39; DOI
530 10.1016/j.jenvrad.2012.11.011.
- 531 (31) Zhang, L.; Zhou, W.; Hou, X.; Chen, N.; Liu, Q.; He, C.; Fan, Y.; Luo, M.; Wang, Z.; Fu, Y.
532 Level and source of ¹²⁹I of environmental samples in Xi'an region, China. *Science of the Total*
533 *Environment*. **2011**, 409(19), 3780-3788; DOI 10.1016/j.scitotenv.2011.06.007.
- 534 (32) Hou, X.; Aldahan, A.; Nielsen, S. P.; Possnert, G. Time series of ¹²⁹I and ¹²⁷I speciation in
535 precipitation from Denmark. *Environmental Science & Technology*. **2009**, 43, 6522-6528; DOI
536 10.1021/es9012678.
- 537 (33) Hou, X.; Hansen, V.; Aldahan, A.; Possnert, G.; Lind, O. C.; Lujaniene, G. A review on
538 speciation of iodine-129 in the environmental and biological samples. *Analytica Chimica Acta*. **2009**,
539 632, 181-196; DOI 10.1016/j.aca.2008.11.013.
- 540 (34) Li, Y.; Li, X.; Xiao, Y.; Zhao, B.; Wang, L. Advances in study on mechanism of foliar nutrition
541 and development of foliar fertilizer application. *Scientia Agricultura Sinica*. **2009**, 42(1), 162-172;
542 DOI 10.3864/j.issn.0578-1752.2009.01.020.
- 543 (35) Xu, S.; Cook, G. T.; Cresswell, A. J.; Dunbar, E.; Freeman, S. P.; Hou, X.; Jacobsson, P.; Kinch,
544 H. R.; Naysmith, P.; Sanderson, D. C.; Tripney, B. G. Radiocarbon Releases from the 2011
545 Fukushima Nuclear Accident. *Sci.Rep*. **2016**, 6, 36947-369752; DOI 10.1038/srep36947.

- 546 (36) Wang, X.; Wang, C.; Zhang, Q.; Li, S.; Li, G. Growth characteristics of heartwood and sapwood
547 of the major tree species in Northeast China. *Science Silvae Sinicae*. **2008**, *44*(5), 102-108; DOI
548 10.11707/j.1001-7488.20080520.
- 549 (37) Eder, M.; Jungnikl, K.; Burgert, I. A close-up view of wood structure and properties across a
550 growth ring of Norway spruce (*Picea abies*[L] Karst.). *Trees*. **2009**, *23*(1), 79-84; DOI
551 10.1007/s00468-008-0256-1.
- 552 (38) Molder, I. European beech grows better and is less drought sensitive in mixed than in pure stands:
553 tree neighbourhood effects on radial increment. *Trees*. **2014**, *28*(3), 777-792; DOI 10.1007/s00468-
554 014-0991-4.
- 555 (39) *NOAA: State of the Climate Report, Climate Monitoring*; National Oceanic and Atmospheric
556 Administration: Washington, DC; <https://www.ncdc.noaa.gov>.
- 557 (40) Young, P.; Archibald, A.; Bowman, K. Pre-industrial to end ²¹th century projections of
558 tropospheric ozone from the Atmospheric Chemistry and Climate Model Intercomparison Project
559 (ACCMIP). *Atmospheric Chemistry and Physics*. **2013**, *13*(4), 2063-2090; DOI 10.5194/acp-13-
560 2063-2013.
- 561 (41) Cooper, O.; Parrish, D.; Ziemke, J. Global distribution and trends of tropospheric ozone: An
562 observation-based review. *Elem Sci Anth*. **2014**, *2*, 29-39; DOI 10.12952/journal.elementa.000029.
- 563 (42) Esen, A. N.; et al.. An overview of energy technologies for a sustainable future. In *Energy*
564 *Systems and Management*; Bilge A., Toy A., Gunay M., Eds.; Springer, Cham: Istanbul 2014; pp 13.
- 565 (43) Wu, X.; Gao, Y.; Guo, Y.; Wu, J. Pollution characteristics of bromine and iodine as trace element
566 in atmospheric particles in Shanghai Caohejing region. *Jornal of Shanghai Normal University*
567 (*Nature Science*). **2009**, *38*(2), 203-209; DOI 10.3969/j.issn.1000-5137.2009.02.016.
- 568 (44) Liao, H.; Bu, W.; Zheng, J.; Wu, F.; Yamada, M. Vertical distributions of radionuclides (²³⁹⁺²⁴⁰Pu,
569 ²⁴⁰Pu/²³⁹Pu, and ¹³⁷Cs) in sediment cores of Lake Bosten in Northwestern China. *Environmental*
570 *Science & Technology*. **2014**, *48*(7), 3840-3846; DOI 10.1021/es405364m.

- 571 (45) Stein, A. F.; Draxler, R. R.; Rolph, G. D.; Stunder, B. J. B.; Cohen, M. D.; Ngan, F. NOAA's
572 HYSPLIT atmospheric transport and dispersion modeling system, *Bull. Amer. Meteor. Soc.*, **2015**, 96,
573 2059-2077; DOI <http://dx.doi.org/10.1175/BAMS-D-14-00110.1>.
- 574 (46) Xu, H.; Wei, J.; Yan, Z.; Zou, W. Influence evaluation of Chernobyl accident in Xinjiang by ^{131}I
575 measured in milk, breast milk and pasture. *Chinese journal of public health*. **1989**, 5(7), 18-20.
- 576 (47) Zhang, J.; Zou, W.; Xu, H.; Wei, J. The total β activity of atmospheric fallouts and aerosols in
577 Xinjiang Province after Chernobyl accident. *Environmental Protection of Xinjiang*. **1987**, 2, 50-57.
- 578 (48) Hou, X.; Povinec, P.; Zhang, L.; Shi, K.; Biddulph, D.; Chang, C.; Fan, Y.; Golser, R.; Hou, Y.;
579 Jeskovsky, M.; Jull, A. J.; Liu, Q.; Luo, M.; Steier, P.; Zhou, W. Iodine-129 in seawater offshore
580 Fukushima: distribution, inorganic speciation, sources, and budget. *Environmental Science &*
581 *Technology*. **2013**, 47(7), 3091-3098; DOI 10.1021/es304460k.
- 582 (49) Tang, M.; Tsuang, B.; Kuo, P. H. Dose estimation for nuclear power plant 4 accident in Taiwan at
583 Fukushima nuclear meltdown emission level. *Journal of Environmental Radioactivity*. **2016**, 155-156,
584 71-83; DOI 10.1016/j.jenvrad.2016.01.022.
- 585 (50) Wang, L.; Zheng, G.; Zhao, S.; Kuo, S.; Xu, M.; Wang, X. Impact of Fukushima Nuclear
586 Accident to China's mainland environment. *Radiation Protection*. **2012**, 32(6), 325-335.
- 587 (51) Zheng, J.; Togami, K.; Watanabe, Y.; Uchida, S.; Aono, T.; Nobuyoshi, I.; Yoshida, S.; Kubota,
588 Y.; Fuma, S.; Ihara, S. Isotopic evidence of plutonium release into the environment from the
589 Fukushima DNPP accident. *Scientific Reports*. **2012**, 2(3), 304-312; DOI 10.1038/srep00304.
- 590 (52) Fan, Y. Spatial distribution of ^{129}I in Chinese surface soil and preliminary study on the ^{129}I
591 chronology. Ph.D. Dissertation, Chinese Academy of Sciences (Institute of Earth Environment
592 Science), Beijing, 2013.
- 593 (53) Englund, E.; Aldahan, A.; Hou, X.; Possnert, G.; Soderstrom, C. Iodine (^{129}I and ^{127}I) in aerosols
594 from northern Europe. *Nuclear Instruments & Methods in Physics Research*. **2010**, 268, 1139-1141;
595 DOI 10.1016/j.nimb.2009.10.118.

596 (54) Jiang, X. A study on the level and variation of ^{129}I in precipitation in Xi'an region and its
597 application as environmental tracer. M.S. Dissertation. Chinese Academy of Sciences (Institute of
598 Earth Environment Science), Beijing, 2017.

599

600

601 **Caption of the figures**

602 Fig. 1 Wood disks of PC1 tree (up) and PC2 tree (bottom), showing the annual rings

603 Fig. 2 Comparison of measured ^{127}I concentrations (a) and $^{129}\text{I}/^{127}\text{I}$ ratios (b) in the tree rings
604 in this work with the reported values in other locations^{16,17, 23, 24}

605 Fig. 3 Temporal variation of the measured $^{129}\text{I}/^{127}\text{I}$ ratios in the tree rings from two sites in the
606 QTP (a), in comparison with the reported variation of $^{129}\text{I}/^{127}\text{I}$ in atmospheric fallout from
607 Tokyo (b)²⁷, yield of fission NWTs (c), yield of thermonuclear weapons tests at Lop Nor
608 (d)²⁰, air releases of ^{129}I from major NFRPs (e) and marine discharges of ^{129}I from
609 NFRPs (f).³³

610 Fig. 4 Variation of iodine (^{127}I) concentration in PC1 and PC2 tree (a), in comparison with the
611 temporal variation of iodine concentrations in ice core in Greenland³

612